Photonic bands in simple and body-centered-cubic cholesteric blue phases

R. M. Hornreich and S. Shtrikman
Department of Electronics, Weizmann Institute of Science, 76100 Rehovot, Israel

C. Sommers
Laboratoire de Physique des Solides, Université de Paris–Sud, Bâtiment 510, F-91405 Orsay CEDEX, France
(Received 23 June 1992)

A procedure is developed for calculating photon bands in materials characterized by tensor dielectric properties. As a specific example, the cholesteric blue phases are considered, and their respective photon bands are calculated for simple and body-centered-cubic structures. These noncentrosymmetric materials interact strongly with only one of the two possible circularly polarized radiation modes; however, no full photon gaps are found even for this mode. The reasons for this are noted. The technique presented is general and can be applied to all materials characterized by tensor dielectric properties.

PACS number(s): 41.20.Bt, 61.30.−v, 71.25.Cx

I. INTRODUCTION

In the past few years, there has been a series of theoretical and experimental studies [1–6] of photonic band states in three-dimensional periodic dielectric solids. One of the motivations for this work has been the possibility of finding or preparing structures in which there are "photonic band gaps," i.e., frequency regions in which the photon density of states is zero. In such energy regions, electromagnetic wave propagation is forbidden and there have been suggestions [1,7,8] as to how this property could be utilized to explore electromagnetic bound states and to improve quantum electronic devices. However, since the desired gaps are at optical frequencies, ordinary solids are not suitable for obtaining such effects. Experimental studies and simulations have therefore concentrated on periodic assemblies of isotropic dielectric spheres, with the filling factor and dielectric constant ratio between the spheres and the uniform background serving as parameters.

Here we introduce a different possibility—that of obtaining photon gaps in materials having tensor dielectric properties. As a specific example of such materials, we consider the so-called cholesteric blue phases (BP). These exist in a narrow temperature region between the disordered and usual helicoidal phases when the cholesteric pitch is sufficiently short [9,10]. Two structures have been identified: simple cubic O^2 ($P4_232$) and body-centered-cubic O^8 ($I4_132$). [A second body-centered structure, O^5 ($I432$), has been discussed, but not observed.] These phases are particularly interesting as (a) their unit-cell size is comparable with optical wavelengths so that they interact strongly with visible radiation, (b) they lack a center of symmetry and are therefore sensitive to the sense of circular polarization of propagating plane waves, and (c) they are naturally existing phases. We emphasize, however, that the method to be employed is applicable to all materials characterized by dielectric tensors.

II. THE BASIC MODEL FOR ANISOTROPIC SYSTEM

The calculation of photonic states anisotropic systems such as BP is, in principle, the same as for simple isotropic dielectrics; one seeks solutions of Maxwell's equations for transverse waves in a periodic structure. However, there is a fundamental difference—the dielectric properties *cannot* be characterized by a simple position-dependent isotropic constant $\epsilon(\mathbf{r})$. Rather, a full *tensor* description $\epsilon_{ij}(\mathbf{r})$ $(i,j=1,2,3)$ is required [10]. We therefore begin with a short derivation of the relevant equations.

For our purposes, the most convenient approach is that of Ho, Chan, and Soukoulis [6], where $\mathbf{H}(\mathbf{r},t)$ [which is equal to $\mathbf{B}(\mathbf{r},t)$ as we ignore the small diamagnetism] is chosen as the basic electromagnetic field vector. Then, taking $\mathbf{H}(\mathbf{r},t)=\mathbf{H}(\mathbf{r})e^{i\omega t}$, etc., we have from Maxwell's equations,

$$\nabla\times\mathbf{H}=-\frac{i\omega}{c}\mathbf{D}=-\frac{i\omega}{c}[\epsilon]\mathbf{E}\ , \tag{1a}$$

$$\nabla\times([\epsilon^{-1}]\nabla\times\mathbf{H})=-\frac{i\omega}{c}\nabla\times\mathbf{E}=\frac{\omega^2}{c^2}\mathbf{H}\ . \tag{1b}$$

All field vectors are now functions of $\mathbf{r}$ only. Since $\nabla\cdot\mathbf{B}=\nabla\cdot\mathbf{H}=0$, $\mathbf{H}$ is a transverse wave. (This is *not* the case for $\mathbf{E}$.) As noted, the permittivity $[\epsilon]$ and its inverse $[\epsilon^{-1}]$ are tensors. In reciprocal space, we have

$$\mathbf{H}(\mathbf{r})=\sum_{\mathbf{G}}\sum_{\lambda=1,2}h_{\mathbf{G},\lambda}\hat{\xi}_\lambda e^{i(\mathbf{K}+\mathbf{G})\cdot\mathbf{r}}\ , \tag{2}$$

where $\{\mathbf{G}\}$ is the group of reciprocal lattice vectors for the space group of interest, $\mathbf{K}$ is a wave vector in the first Brillouin zone, $\hat{\xi}_1,\hat{\xi}_2$, and $(\mathbf{K}+\mathbf{G})$ form a local right-handed coordinate system, and the $h_{\mathbf{G},\lambda}$ are Fourier amplitudes. We also expand $[\epsilon^{-1}(\mathbf{r})]$ in reciprocal space, obtaining

$$[\epsilon^{-1}(\mathbf{r})]=\sum_{\mathbf{G}}[\epsilon^{-1}]_{\mathbf{G}}e^{i\mathbf{G}\cdot\mathbf{r}}$$
$$=\sum_{\mathbf{G}}\sum_{\alpha,\beta=1,2,3}\epsilon^{-1}_{\alpha\beta}(\mathbf{G})\hat{e}_\alpha\hat{e}_\beta e^{i\mathbf{G}\cdot\mathbf{r}}\ . \quad (3)$$

Here the tensor $[\epsilon^{-1}]_{\mathbf{G}}$ is the Fourier transform of $[\epsilon^{-1}(\mathbf{r})]$ and $\epsilon^{-1}_{\alpha\beta}(\mathbf{G})$ are its elements in a local right-handed coordinate system defined by $\hat{\mathbf{e}}_1$, $\hat{\mathbf{e}}_2$, and $\hat{\mathbf{e}}_3=\mathbf{G}/|\mathbf{G}|$. [We stress the *local* character of the coordinate systems in (2) and (3); they are defined independently for *each* of the wave vectors appearing in the Fourier sums.] The right-hand side of (3) is written in dyadic notation.

Substituting (2) and (3) into (1b) formally transforms a linear differential equation for $\mathbf{H}(\mathbf{r})$ into a matrix equation for the $\{h_{\mathbf{G},\lambda}\}$. The latter has the form

$$\sum_{\mathbf{G}'}\sum_{\lambda'=1,2}F^{\lambda,\lambda'}_{\mathbf{G},\mathbf{G}'}h_{\mathbf{G}',\lambda'}=\frac{\omega^2}{c^2}h_{\mathbf{G},\lambda}\ , \quad (4)$$

where $F^{\lambda,\lambda'}_{\mathbf{G},\mathbf{G}'}$ are the elements of a 2×2 tensor $[F_{\mathbf{G},\mathbf{G}'}]$ which is given by

$$[F_{\mathbf{G},\mathbf{G}'}]=\sum_{\alpha,\beta}|\mathbf{K}+\mathbf{G}||\mathbf{K}+\mathbf{G}'|\epsilon^{-1}_{\alpha\beta}(\mathbf{G}-\mathbf{G}')$$
$$\times\begin{bmatrix}\hat{\xi}_1\cdot\hat{\mathbf{e}}_\alpha\hat{\mathbf{e}}_\beta\cdot\hat{\xi}_{1'} & -\hat{\xi}_1\cdot\hat{\mathbf{e}}_\alpha\hat{\mathbf{e}}_\beta\cdot\hat{\xi}_{2'}\\ -\hat{\xi}_2\cdot\hat{\mathbf{e}}_\alpha\hat{\mathbf{e}}_\beta\cdot\hat{\xi}_{1'} & \hat{\xi}_2\cdot\hat{\mathbf{e}}_\alpha\hat{\mathbf{e}}_\beta\cdot\hat{\xi}_{2'}\end{bmatrix}\ . \quad (5)$$

Here $\hat{\xi}_1,\hat{\xi}_2$ and $\hat{\xi}_{1'},\hat{\xi}_{2'}$ denote local axes associated with the wave vectors $(\mathbf{K}+\mathbf{G})$ and $(\mathbf{K}+\mathbf{G}')$, respectively, and $\hat{\mathbf{e}}_\alpha,\hat{\mathbf{e}}_\beta$ are associated with the reciprocal lattice vector $\mathbf{G}''=\mathbf{G}-\mathbf{G}'$. Comparing our Eq. (5) with that of Ho, Chan, and Soukoulis [6] makes clear the effect of the medium having tensor rather than scalar dielectric properties.

III. PHOTON BANDS IN BLUE PHASES

A. General considerations

Physically, it is unlikely that a full photon gap will occur in cholesteric systems. This is inherent in the chiral nature of these materials—they interact very strongly only with radiation having a particular circular polarization and very weakly with the opposite polarization [9,10]. Thus a gap would in all likelihood exist, if at all, only for one sense of circular polarization. This polarization dependence is not characteristic of all tensor dielectric systems but only of those which are, in addition, noncentrosymmetric.

In order to solve the secular equation $|F^{\lambda,\lambda'}_{\mathbf{G},\mathbf{G}'}-(\omega^2/c^2)\delta_{\mathbf{G},\lambda;\mathbf{G}',\lambda'}|=0$ and obtain the photonic bands, the Fourier elements $\epsilon^{-1}_{\alpha\beta}(\mathbf{G})$ of the inverse dielectric tensor associated with each reciprocal lattice vector of the structure are needed. For the BP, these are available from earlier calculations of the phase diagram of cholesteric systems, wherein the ratios of the Fourier elements of the anisotropic part of the dielectric tensor were determined by minimizing free energies for the cubic structures [11]. Although there $[\epsilon]$ was used as the order parameter in the Landau–de Gennes free-energy expansion, $[\epsilon^{-1}]$ would have served equally as well. Thus the element ratios found for $[\epsilon]_{\mathbf{G}}$ are equally valid for $[\epsilon^{-1}]_{\mathbf{G}}$.

To connect with the free-energy studies, we note that the anisotropic part of the normalized order-parameter tensor was taken as [11]

$$[\mu_{ij}(\mathbf{r})]=\sum_{h,k,l}N^{-1/2}[\mu_{ij}(\sigma)]\exp[iq(hx+ky+lz)]\ , \quad (6)$$

with h,k,l Miller indices, $\sigma=h^2+k^2+l^2$, $N=3!2^{3-n_0}/n_1!$, where $n_0(n_1)$ is the number of vanishing (equal) $|h|,|k|,|l|$ and, for each $[hkl]$,

$$[\mu(\sigma)]=\sum_{m=-2}^{2}\mu_m(\sigma)e^{i\psi_m(hkl)}[M_m(hkl)]$$
$$=\frac{1}{2}\left\{\mu_2e^{i\psi_2}\begin{bmatrix}1&i&0\\i&-1&0\\0&0&0\end{bmatrix}+\mu_1e^{i\psi_1}\begin{bmatrix}0&0&1\\0&0&i\\1&i&0\end{bmatrix}+\left[\frac{2}{3}\right]^{1/2}\mu_0e^{i\psi_0}\begin{bmatrix}-1&0&0\\0&-1&0\\0&0&2\end{bmatrix}\right.$$
$$\left.+\mu_{-1}e^{i\psi_{-1}}\begin{bmatrix}0&0&-1\\0&0&i\\-1&i&0\end{bmatrix}+\mu_{-2}e^{i\psi_{-2}}\begin{bmatrix}1&-i&0\\-i&-1&0\\0&0&0\end{bmatrix}\right\}\ , \quad (7)$$

with $\mu_m(\sigma)\geq0$ and $\psi_m(hkl)=-\psi_m(\bar{h}\,\bar{k}\,\bar{l})$. The $[M_m]$ basis matrices are defined such that $[hkl]$ is the polar axis of a local coordinate system, defined separately for each $[hkl]$. Further, the lowest-lying states lie on either the $m=+2$ or -2 branch of the free energy versus wave-vector spectrum, depending upon the chirality (left or right handed) of the system. Taking only $m=+2$ states, we have

$$[\mu_{ij}(\mathbf{r})]=\tfrac{1}{2}\sum_{h,k,l}N^{-1/2}\mu_2(\sigma)e^{i\psi_2(hkl)}(\hat{\mathbf{e}}_1+i\hat{\mathbf{e}}_2)(\hat{\mathbf{e}}_1+i\hat{\mathbf{e}}_2)$$
$$\times\exp[iq(hx+ky+lz)]\ . \quad (8)$$

This expression can be compared directly with (3). Of course, the isotropic part of the order parameter must also be included. Its Fourier transform is at $\mathbf{G}=0$ and is

proportional to the unit tensor $\delta_{\alpha\beta}$ (or, equivalently, the unit dyadic $\hat{\mathbf{e}}_\alpha\hat{\mathbf{e}}_\alpha$). Thus it contributes only to the main diagonal elements of $F^{\lambda,\lambda'}_{\mathbf{G},\mathbf{G}'}$, giving

$$F^{\lambda,\lambda}_{\mathbf{G},\mathbf{G}}=|\mathbf{K}+\mathbf{G}|^2\epsilon^{-1}(0)\ . \tag{9}$$

Note, from (4), that $\epsilon^{-1}(0)$ may be taken as a scale factor for (ω^2/c^2). This then fixes the values of the scaled anisotropic elements $\mu_2(\sigma)$, whose ratios are, as noted, given by the free-energy minimization. Moreover, as these elements are (α,β) independent, we may use (8) to simplify (5) to

$$[F_{\mathbf{G},\mathbf{G}'}]=\frac{1}{2\sqrt{N}}|\mathbf{K}+\mathbf{G}||\mathbf{K}+\mathbf{G}'|\mu_2(G'')e^{i\psi_2(\mathbf{G}'')} \times\begin{bmatrix}\hat{\xi}_1\cdot(\hat{\mathbf{e}}_{1''}+i\hat{\mathbf{e}}_{2''})\\ \hat{\xi}_2\cdot(\hat{\mathbf{e}}_{1''}+i\hat{\mathbf{e}}_{2''})\end{bmatrix} \times[\hat{\xi}_{1'}\cdot(\hat{\mathbf{e}}_{1''}+i\hat{\mathbf{e}}_{2''})\hat{\xi}_{2'}\cdot(\hat{\mathbf{e}}_{1''}+i\hat{\mathbf{e}}_{2''})]\ , \tag{10}$$

where $\hat{\mathbf{e}}_{1''},\hat{\mathbf{e}}_{2''}$ are associated with the vector $\mathbf{G}''=\mathbf{G}-\mathbf{G}'$.

In our numerical calculations, the **H**-field basis vector sets $\{\hat{\xi}_i\}$ were generated by choosing a unit vector $\hat{\mathbf{u}}$, *not* parallel (but otherwise arbitrary) to any of the vectors $\{\mathbf{K}+\mathbf{G}\}$. Then

$$\hat{\xi}_1=\hat{\mathbf{u}}\times(\mathbf{K}+\mathbf{G})/(K+G)\ ,\quad \hat{\xi}_2=(\mathbf{K}+\mathbf{G})\times\hat{\xi}_1/(K+G)\ . \tag{11}$$

The basis vector sets $\{\hat{\mathbf{e}}_i\}$ and phases $\{\psi_2\}$ associated with the Fourier components of the order parameter are determined by the space-group symmetry characterizing each of the cubic BP [11].

B. Simple cubic O^2: Blue phase II

BPII is characterized by the sc space group O^2 ($P4_232$) [9–11]. Free-energy calculations [11] have established that this phase is well represented by an order parameter with two nonzero Fourier amplitudes, $\mu_2(1)$ and $\mu_2(2)$, associated with the reciprocal wave-vector sets $\langle 100\rangle$ and $\langle 110\rangle$, respectively. The phases [with respect to an origin at the point (000) in the O^2 crystallographic cell with point-group symmetry 23] are $\psi_2(\langle 100\rangle)=0$ and $\psi_2(\langle 110\rangle)=\pi$. These phases are identical for all wave vectors belonging to a given set. Representative values for the normalized amplitudes are $\mu_2(1)=0.5$ and $\mu_2(2)=0.3$.

In order to determine the absolute values of these amplitudes, we used the following approach: In nematic liquid crystals (or racemic mixtures of cholesteric liquid crystals), the value of the normalized order parameter at the phase transition, $\mu_N=0.5$, is related to the difference between the dielectric constants parallel ($\epsilon_\parallel$) and perpendicular ($\epsilon_\perp$) to the nematic axis by [10,11] $f\mu_N/\epsilon(0)=\sqrt{6}\Delta\epsilon/3\epsilon_{\rm av}$, where $\Delta\epsilon=|\epsilon_\parallel-\epsilon_\perp|$ and $\epsilon(0)=\epsilon_{\rm av}=(\epsilon_\parallel+2\epsilon_\perp)/3$. The scaling parameter f will be assumed to be structure independent. Typical values [12] at optical frequencies for $(\Delta\epsilon/\epsilon_{\rm av})$ are about 0.40, which gives $f=0.6$. We then have for the two nonzero scaled [with respect to $\epsilon^{-1}(0)$] amplitudes,

$$\frac{1}{2\sqrt{N}}f\mu_2(1)=\frac{1}{2\sqrt{6}}(0.6)(0.5)=0.06\ ,\qquad \frac{1}{2\sqrt{N}}f\mu_2(2)=\frac{1}{2\sqrt{12}}(0.6)(0.3)=0.03\ . \tag{12}$$

The basis vector sets $\{e_i\}$ have been determined elsewhere [11] and are summarized in Table I.

Using the above parameters, we have constructed $F^{\lambda,\lambda'}_{\mathbf{G},\mathbf{G}'}$ matrices up to 294×294 (i.e., 147 plane waves and two polarizations). Low-lying eigenvalues were calculated and the resulting photon band structure on the symmetry axes is shown in Fig. 1(a). We also give, for comparison, the results of a calculation using Fourier amplitudes three times larger in Fig. 1(b). We shall discuss these results in Sec. IV.

C. Body-centered-cubic O^5

This structure, which may exist for sufficiently short cholesteric pitch [10,13], has not been observed experimentally. However, as it is relatively simple and may be of future interest, we have calculated its photon band states also.

For the case of bcc O^5 (I432), there is only a single relevant Fourier amplitude $\mu_2(2)$ associated with the reciprocal wave-vector set $\langle 110\rangle$. The phases $\psi_2=0$ for all these wave vectors. The scaled amplitude is here

$$\frac{1}{2\sqrt{N}}f\mu_2(2)=\frac{1}{2\sqrt{12}}(0.6)(0.45)=0.04\ . \tag{13}$$

TABLE I. Reciprocal lattice vectors and their associated local axes $\hat{\mathbf{e}}_1,\hat{\mathbf{e}}_2$. The sets [$\langle 100\rangle$, $\langle 110\rangle$], [$\langle 110\rangle$], and [$\langle 110\rangle,\langle 200\rangle,\langle 211\rangle$] are relevant for sc O^2, bcc O^5, and bcc O^8, respectively. For the inverses of the vectors given in the table, replace $\hat{\mathbf{e}}_2$ by $-\hat{\mathbf{e}}_2$.

Wave vector	$\hat{\mathbf{e}}_1$	$\hat{\mathbf{e}}_2$
[100];[200]	$\hat{\mathbf{y}}$	$\hat{\mathbf{z}}$
[010];[020]	$\hat{\mathbf{z}}$	$\hat{\mathbf{x}}$
[001];[002]	$\hat{\mathbf{x}}$	$\hat{\mathbf{y}}$
[110]	$\hat{\mathbf{z}}$	$(\hat{\mathbf{x}}-\hat{\mathbf{y}})/\sqrt{2}$
[011]	$\hat{\mathbf{x}}$	$(\hat{\mathbf{y}}-\hat{\mathbf{z}})/\sqrt{2}$
[101]	$\hat{\mathbf{y}}$	$(\hat{\mathbf{z}}-\hat{\mathbf{x}})/\sqrt{2}$
[$\bar{1}$10]	$-\hat{\mathbf{z}}$	$-(\hat{\mathbf{x}}+\hat{\mathbf{y}})/\sqrt{2}$
[0$\bar{1}$1]	$-\hat{\mathbf{x}}$	$-(\hat{\mathbf{y}}+\hat{\mathbf{z}})/\sqrt{2}$
[10$\bar{1}$]	$-\hat{\mathbf{y}}$	$-(\hat{\mathbf{z}}+\hat{\mathbf{x}})/\sqrt{2}$
[211]	$-(\hat{\mathbf{x}}+\hat{\mathbf{y}}+\hat{\mathbf{z}})/\sqrt{3}$	$(\hat{\mathbf{y}}-\hat{\mathbf{z}})/\sqrt{2}$
[121]	$-(\hat{\mathbf{x}}+\hat{\mathbf{y}}+\hat{\mathbf{z}})/\sqrt{3}$	$(\hat{\mathbf{z}}-\hat{\mathbf{x}})/\sqrt{2}$
[112]	$-(\hat{\mathbf{x}}+\hat{\mathbf{y}}+\hat{\mathbf{z}})/\sqrt{3}$	$(\hat{\mathbf{x}}-\hat{\mathbf{y}})/\sqrt{2}$
[2$\bar{1}$1]	$(\hat{\mathbf{y}}-\hat{\mathbf{z}}+\hat{\mathbf{x}})/\sqrt{3}$	$(\hat{\mathbf{y}}+\hat{\mathbf{z}})/\sqrt{2}$
[12$\bar{1}$]	$(\hat{\mathbf{z}}-\hat{\mathbf{x}}+\hat{\mathbf{y}})/\sqrt{3}$	$(\hat{\mathbf{z}}+\hat{\mathbf{x}})/\sqrt{2}$
[$\bar{1}$12]	$(\hat{\mathbf{x}}-\hat{\mathbf{y}}+\hat{\mathbf{z}})/\sqrt{3}$	$(\hat{\mathbf{x}}+\hat{\mathbf{y}})/\sqrt{2}$
[21$\bar{1}$]	$(-\hat{\mathbf{y}}+\hat{\mathbf{z}}+\hat{\mathbf{x}})/\sqrt{3}$	$-(\hat{\mathbf{y}}+\hat{\mathbf{z}})/\sqrt{2}$
[$\bar{1}$21]	$(-\hat{\mathbf{z}}+\hat{\mathbf{x}}+\hat{\mathbf{y}})/\sqrt{3}$	$-(\hat{\mathbf{z}}+\hat{\mathbf{x}})/\sqrt{2}$
[1$\bar{1}$2]	$(-\hat{\mathbf{x}}+\hat{\mathbf{y}}+\hat{\mathbf{z}})/\sqrt{3}$	$-(\hat{\mathbf{x}}+\hat{\mathbf{y}})/\sqrt{2}$
[2$\bar{1}$1]	$(\hat{\mathbf{x}}+\hat{\mathbf{y}}+\hat{\mathbf{z}})/\sqrt{3}$	$(-\hat{\mathbf{y}}+\hat{\mathbf{z}})/\sqrt{2}$
[$\bar{1}$2$\bar{1}$]	$(\hat{\mathbf{x}}+\hat{\mathbf{y}}+\hat{\mathbf{z}})/\sqrt{3}$	$(-\hat{\mathbf{z}}+\hat{\mathbf{x}})/\sqrt{2}$
[$\bar{1}\,\bar{1}$2]	$(\hat{\mathbf{x}}+\hat{\mathbf{y}}+\hat{\mathbf{z}})/\sqrt{3}$	$(-\hat{\mathbf{x}}+\hat{\mathbf{y}})/\sqrt{2}$

The set $\{e_i\}$ for the $\langle 110 \rangle$ reciprocal lattice vectors are given in Table I.

Using the amplitude given in (13), we have constructed $F^{\lambda,\lambda'}_{G,G'}$ matrices up to 282×282 (i.e., 141 plane waves and two polarizations). As before, low-lying eigenvalues were calculated on symmetry axes of the unit cell; the resulting photon bands are shown in Fig. 2(a). We also give the results for a Fourier amplitude three times larger in Fig. 2(b). These results will be discussed in Sec. IV.

D. Body-centered-cubic O^8: Blue phase I

The BPI structure belongs to the bcc space groups O^8 ($I4_132$) [9–11]. It is more complex that the two groups described earlier and at least three nonzero Fourier amplitudes are needed in its order parameter. These are associated with the reciprocal wave-vector sets $\langle 110 \rangle$, $\langle 200 \rangle$, and $\langle 211 \rangle$ and will be labeled $\mu_2(2)$, $\mu_2(4)$, and $\mu_2(6)$, respectively. [In the free-energy calculations, a fourth amplitude, associated with $\langle 220 \rangle$, was also considered [11]. It was found to be much smaller than the other three and we shall neglect it here.] The phases [all with respect to the point $(\frac{1}{8}\frac{1}{8}\frac{1}{8})$ of the crystallographic unit with symmetry 32] are as follows:

$$\begin{aligned} &\psi_2(110) = -\psi_2(\bar{1}10) - \tfrac{1}{2}\pi = 0 , \\ &\psi_2(200) = -\tfrac{1}{2}\pi , \\ &\psi_2(211) = \psi_2(2\bar{1}1) - \tfrac{1}{2}\pi = -\psi_2(21\bar{1}) - \tfrac{1}{2}\pi \\ &\qquad\qquad = \psi_2(2\bar{1}\bar{1}) = 0 . \end{aligned} \tag{14}$$

All other phases may be found from (14) by cyclic permutation and the relation $\psi_2(hkl) = -\psi_2(\bar{h}\,\bar{k}\,\bar{l})$. For the amplitudes, the free-energy minimization results [11] are equivalent to

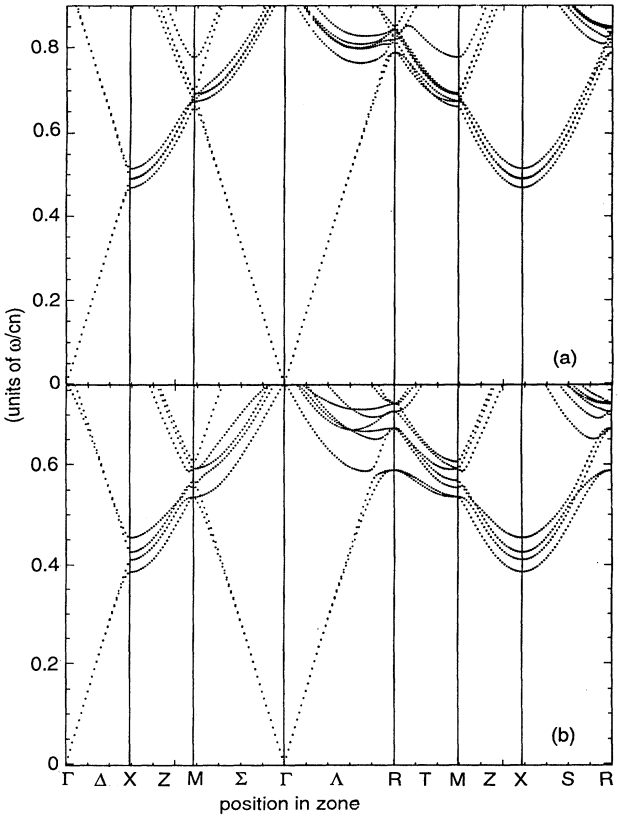

FIG. 1. Photon bands in the simple cubic structure O^2 ($P4_232$) with dielectric tensor components (a) appropriate to cholesteric blue phase II (b) three times larger than in (a). The energy is given as a function of wave vector on the special lines in the first Brillouin zone in units of ω/cn, where $n = \sqrt{\epsilon_{av}}$ is the average index of refraction. The band gaps relevant to optical frequencies are between the first and fourth bands (with increasing energy) for the circular polarized radiation mode strongly interacting with the material and between the second and third for the oppositely polarized mode.

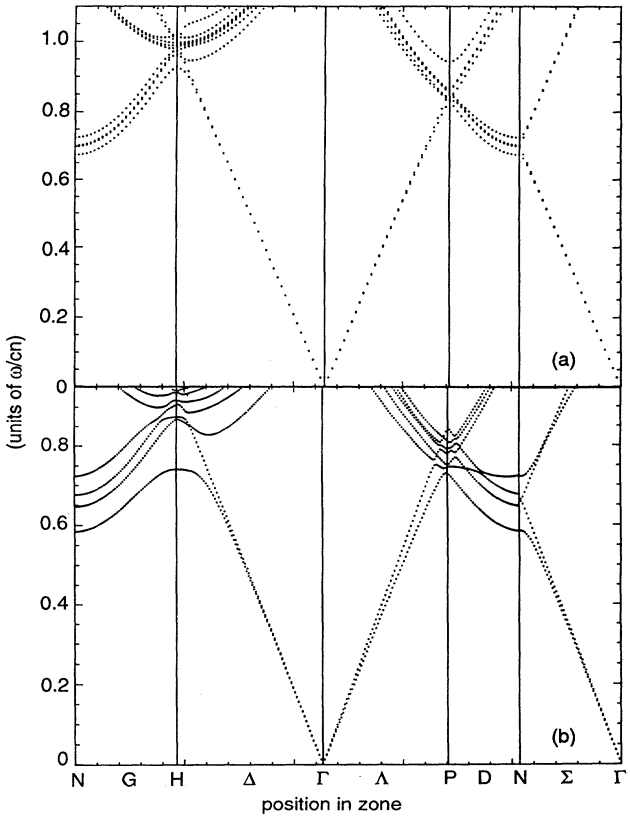

FIG. 2. Photon bands in the body-centered-cubic structure O^5 ($I432$) with dielectric tensor components (a) appropriate to the free-energy minimization for this structure (b) three times larger than in (a). The energy is given as a function of wave vector on the special lines in the first Brillouin zone in units of ω/cn, where $n = \sqrt{\epsilon_{av}}$ is the average index of refraction. The band gaps relevant to optical frequencies are between the first and fourth bands (with increasing energy) for the circular polarized radiation mode strongly interacting with the material and between the second and third for the oppositely polarized mode.

$$\frac{1}{2\sqrt{N}} f\mu_2(2) = \frac{1}{2\sqrt{12}}(0.6)(0.60) = 0.05 ,$$
$$\frac{1}{2\sqrt{N}} f\mu_2(4) = \frac{1}{2\sqrt{6}}(0.6)(0.45) = 0.06 , \quad (15)$$
$$\frac{1}{2\sqrt{N}} f\mu_2(6) = \frac{1}{2\sqrt{24}}(0.6)(0.3) = 0.02 .$$

The relevant basis vector sets $\{e_i\}$ are given in Table I.

As for the other structures studied, we used (15) to obtain the $F^{\lambda,\lambda'}_{G,G'}$ matrix. Up to 141 plane waves were used (i.e., the maximum matrix investigated was 282×282) and the low-lying eigenvalues were calculated. The resulting photon bands for points on the symmetry axes are shown in Fig. 3(a) and the results for amplitudes three times larger are given in Fig. 3(b). These will be discussed in the next section.

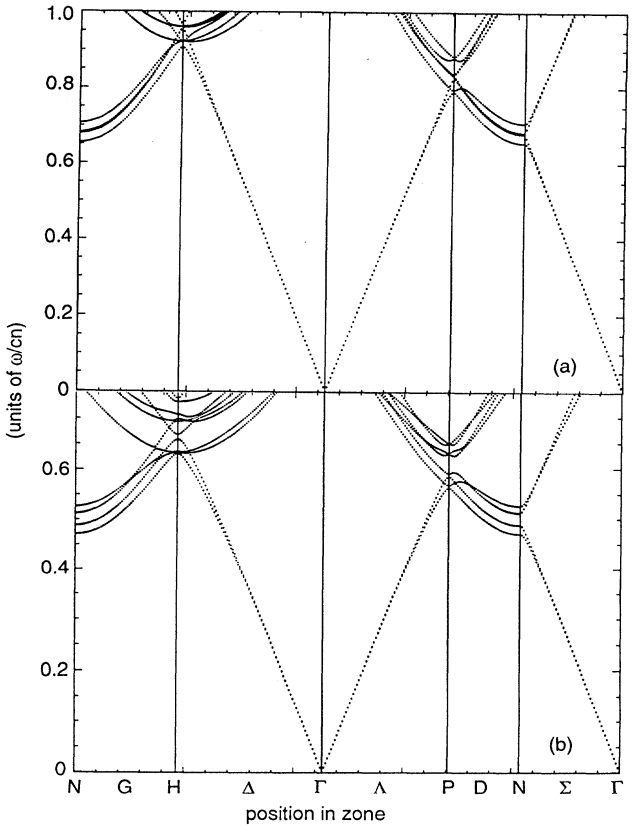

FIG. 3. Photon bands in the body-centered-cubic structure O^8 ($I4_132$) with dielectric tensor components (a) appropriate to cholesteric blue phase I (b) three times larger than in (a). The energy is given as a function of wave vector on the special lines in the first Brillouin zone in units of ω/cn, where $n=\sqrt{\epsilon_{av}}$ is the average index of refraction. The band gaps relevant to optical frequencies are between the first and fourth bands (with increasing energy) for the circular polarized radiation mode strongly interacting with the material and between the second and third for the oppositely polarized mode.

IV. DISCUSSION

In Secs. II and III, we showed how techniques developed to calculate photon bands for materials with scalar dielectric properties can be modified and applied to tensor dielectric systems. In practice, the equations for the band states can be solved via the same approach used earlier—numerical diagonalization of a relatively large matrix whose elements are obtained by expanding the electromagnetic field vectors in a set of plane-wave states. The material parameters enter the calculation via the inverse dielectric tensor, which is expanded in wave vectors of the reciprocal lattice. It is important that the phase factors associated with the Fourier amplitudes be appropriate to the given space group. To illustrate the method and also because of their intrinsic interest, the method was applied to three noncentrosymmetric structures which have been studied in connection with the cubic blue phases (BP) found in cholesteric liquid-crystal systems. Two of these structures [sc O^2 ($P4_232$) and bcc O^8 ($I4_132$)] have been identified [9–11] as characterizing BPII and BPI, respectively, while the third O^5 ($I432$) may eventually be found in very short pitch materials. Two of these structures (O^2 and O^8) are nonsymmorphic.

The low-lying photon bands calculated for these three BP structures are given in parts (a) of Figs. 1–3. In all cases, we see that even at some reciprocal lattice points (e.g., points X and N), there is a gap in the spectrum essentially only for waves with one circular polarization. For the opposite polarization, the gap at these points is negligibly small and cannot be distinguished in the figures. This is in accord with many studies [9] on the selective nature of Bragg backscattering at these wave vectors. However, even for that mode having a gap at the zone edges, we do not find a full photon gap over the entire zone. This is not unexpected given the difficulty in finding such gaps in artificial fcc structures, particularly as the latter have two advantages over BP structures. First, the Brillouin zone for fcc structures is more spherical (i.e., the relative difference in length between the shortest and longest wave vectors from the zone center to the zone boundary is smaller) than for sc or bcc ones. This is a purely geometrical factor. Second, cholesteric liquid crystals have orientational rather than translational order. In such systems, periodic variations in the dielectric properties are basically due to the difference in electric polarizability parallel and perpendicular to the axis of the rodlike molecules rather than to, e.g., the presence or absence of dielectric spheres. The former are intrinsically smaller in magnitude than the latter and, consequently, so are the gaps induced by a periodic potential in the BP at the band edges.

This second point is illustrated in parts (b) of Figs. 1–3. Here we have tripled the amplitude of the periodic part of the dielectric tensor and calculated the resultant photon bands. Even with such dielectric properties (which, of course, are much larger than any found in present-day cholesteric materials) it is clear that we are still far from a full photon band gap, even for one circular polarization only, in the observed BP structures, O^2 and O^8. For O^5, on the other hand, we see from Fig. 2(b) that

a full band gap (for one polarization only) is almost present, the overlap between the two relevant bands (the lowest-lying one at point H and the fourth one at point N) being about 0.04. Thus we may conclude that while polarization-dependent photon band gaps are not likely to occur in the BP, they are not intrinsically impossible. It would therefore be of interest to also consider centrosymmetric materials (e.g., lyotropics, microemulsions, colloidal crystals) in which full photon gaps, if they exist, will not be polarization dependent.

More generally, we have shown that the extension of previous calculations to the case of materials with tensor dielectric properties can be carried out straightforwardly. We have thus opened a way to explore the utilization of such materials in designing structures with full photon band gaps. Given the interest, both fundamental and applied, in finding such structures, these possibilities should be explored further.

ACKNOWLEDGMENTS

C.S. acknowledges the financial support of the Einstein Center for Theoretical Physics of the Weizmann Institute of Science, the hospitality of the Center for Computational Physics of the University of Kentucky, and the technical support of IBM-GEPSI with regard to the RS/6000 computer upon which the numerical calculations were carried out.

[1] E. Yablonovitch, Phys. Rev. Lett. **58**, 2059 (1987).
[2] S. John, Phys. Rev. Lett. **58**, 2486 (1987).
[3] E. Yablonovitch and T. J. Gmitter, Phys. Rev. Lett. **63**, 1950 (1989).
[4] K. M. Leung and Y. F. Lin, Phys. Rev. Lett. **65**, 2646 (1990).
[5] Z. Zhang and S. Satpathy, Phys. Rev. Lett. **65**, 2650 (1990).
[6] K. M. Ho, C. T. Chan, and C. M. Soukoulis, Phys. Rev. Lett. **65**, 3152 (1990).
[7] G. Kurizki and A. Z. Genack, Phys. Rev. Lett. **61**, 2269 (1988).
[8] S. John and J. Wang, Phys. Rev. Lett. **614**, 2418 (1990).
[9] For an experimental review, see P. P. Crooker, Liq. Cryst. **5**, 751 (1989).
[10] For a theoretical review, see R. M. Hornreich and S. Shtrikman, Mol. Cryst. Liq. Cryst. **165**, 183 (1988).
[11] H. Grebel, R. M. Hornreich, and S. Shtrikman, Phys. Rev. A **30**, 3264 (1984).
[12] G. Vertoyen and W. H. de Jeu, *Thermotropic Liquid Crystals, Fundamentals* (Springer, Berlin, 1988), Chap. 10.
[13] D. C. Wright and N. D. Mermin, Phys. Rev. A **31**, 3498 (1985).